Azimuthal Asymmetries in Energy Correlators: Probing Transversity and NGLs

Wanchen Li
wanchen1995@outlook.com

Department of Physics, Fudan University

SCET 2026

KIAS, Seoul, Korea

Mar 2nd, 2026

Based on works:

- Accessing Nucleon Transversity with One-Point Energy Correlators,

  ArXiv: 2509.15809,

  Authors: Mei-Sen Gao, Zhong-Bo Kang, Wanchen Li, Ding-Yu Shao.

- Energy-Energy Correlator Azimuthal Asymmetries from Recoil.

  ArXiv: 2603.xxxxx,

  Authors: Wanchen Li, Yu-Xuan Sun, Ding-Yu Shao.

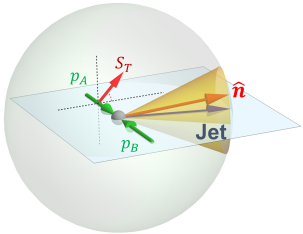

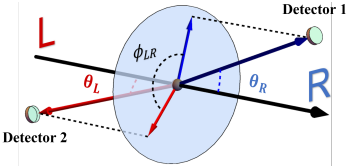

Motivation

- Transversity distribution h_1^q is a fundamental, yet less known, parton distribution.
- Its chiral-odd nature prevents access via inclusive DIS.
- Nucleon tensor charge δq from h_1^q

$$\delta q \equiv \int_0^1 dx \, [h_1^q(x) - h_1^{\bar{q}}(x)]$$

is essential for:

  - Nucleon spin structure,
  - Lattice QCD benchmarks,
    X. Gao, A. D. Hanlon, S. Mukherjee, P. Petreczky, Q. Shi, S. Syritsyn, and Y. Zhao, (2024).
  - BSM probes, e.g. neutron β-decay,
    J. D. Jackson, S. B. Treiman, and H. W. Wyld, (1957).

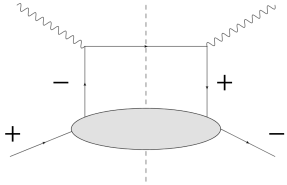

Transversity forbidden in Inclusive DIS

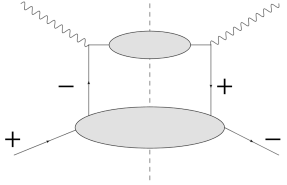

Semi-inclusive DIS (SIDIS)

Jet Production in Transversely Polarized $p^\uparrow p$ Collision

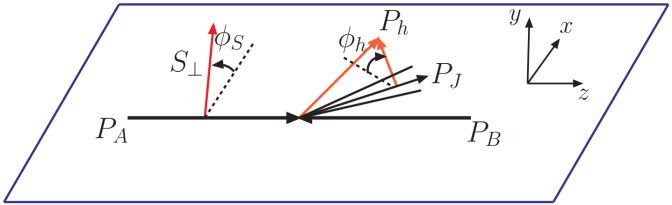

- Proposed by F. Yuan, Phys.Rev.Lett. 100, 032003 (2008), the differential cross section comes with an azimuthal modualtion,

$$\frac{\mathrm{d}\sigma}{\mathrm{d}\mathcal{P}\mathcal{S}} = F_{UU} + \sin\left(\phi_s - \phi_h\right) F_{UT}.$$

- The reaction plane is spanned by the two incoming protons and the jet axis.
  - ϕ_s: the azimuthal angle of transverse polarization vector $S_\perp$, with respect the to reaction plane.
  - ϕ_h: the azimuthal angle of hadron h in jet, with respect the to reaction plane.

One Point Energy Correlator (OPEC)

- We define the infrared-collinear (IRC) safe one-point energy correlator (OPEC) as

$$\Delta^q(z,\hat{\boldsymbol{n}}) = \sum_X \sum_{i\in J} \langle\Omega|\bar{\chi}_n \delta_{Q,\mathcal{P}_n} \delta^{(2)}(\hat{\boldsymbol{n}} - \hat{\boldsymbol{n}}_i)|J(h_i)X\rangle \frac{E_i}{E_J} \langle J(h_i)X|\chi_n|\Omega\rangle,$$

- $\hat{\boldsymbol{n}}$ is the direction of the energy flow.
- The energy fraction of the jet carried by the hadron i is $z_i = \frac{E_i}{E_J}$.
- χ is the gauge-invarinat quark field.
- The state $|JX\rangle$ represents the final-state unobserved particles X and the jet J.

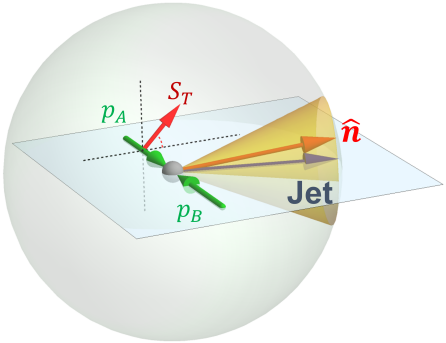

Decomposition of OPEC

- Ignoring irrelevant helicity and transverse components, we decompose OPEC into two parts:

$$\Delta_q^{[\gamma^+]} = \mathcal{J}^q,$$

$$\Delta_q^{[i\sigma^{\alpha+}\gamma_5]} = \epsilon_T^{\alpha\beta}\hat{\boldsymbol{n}}_{T,\beta}\frac{p_J^-}{2}\theta_n\mathcal{J}_{1,\perp}^q,$$

- $\mathcal{J}^q$ is the unpolarized OPEC fragmenting jet function (FJF).
- $\mathcal{J}_{1,\perp}^q$ is the transversely polarized OPEC FJF.
- θ_n is the energy flow polar angle.

Factorization

- We consider the OPEC in inclusive jet production in $p^{\uparrow} + p \to J + X$

$$\frac{\mathrm{d}\Sigma}{\mathrm{d}\theta_n \mathrm{d}\phi_n \mathrm{d}\eta\, \mathrm{d}p_T} = \sum_{h\in J} \int_0^1 \mathrm{d}z_h \int \mathrm{d}^2\Omega_{\boldsymbol{h}}\, \delta\left(\phi_n - \phi_h\right) \times \delta\left(\theta_n - \theta_h\right)\, z_h\, \frac{\mathrm{d}\sigma}{\mathrm{d}z_h\, \mathrm{d}^2\Omega_h \mathrm{d}\eta\, \mathrm{d}p_T}$$

- z_h is the weight factor.
- Integral on z_h converts the final-state z_h distribution into a number!
- The jet is characterized by the rapidity η and transverse momentum p_T.
- The azimuthal dependent OPEC inclusive jet production can be described by

$$\frac{\mathrm{d}\Sigma}{\mathrm{d}\theta_n \mathrm{d}\phi_n \mathrm{d}\eta\, \mathrm{d}p_T} = Z_{UU} + \sin\left(\phi_s - \phi_n\right) Z_{UT}.$$

Factorization with OPEC in Inclusive Jet Production

- The energy-weighted unpolarized and transversely polarized structure functions Z_{UU} and Z_{UT} admit the following factorized forms:

$$
\begin{aligned}
Z_{UU} =& \frac{\alpha_s^2}{s} p_T^2 \theta_n \sum_{a,b,c} \int \frac{\mathrm{d}x_1}{x_1} f_{a/A}(x_1,\mu) \int \frac{\mathrm{d}x_2}{x_2} f_{b/B}(x_2,\mu) \\
& \times \mathcal{J}^c(\theta_n, Q) H^{\mathrm{U}}_{ab\to c}(\hat{s},\hat{t},\hat{u}) \delta(\hat{s}+\hat{t}+\hat{u}) \,, \\
Z_{UT} =& \frac{\alpha_s^2}{s} p_T^2 \theta_n \sum_{a,b,c} \int \frac{dx_1}{x_1} h_1^a(x_1,\mu) \int \frac{dx_2}{x_2} f_{b/B}(x_2,\mu) \\
& \times p_T \theta_n \mathcal{J}^c_{1,\perp}(\theta_n, Q) H^{\mathrm{Collins}}_{ab\to c}(\hat{s},\hat{t},\hat{u}) \delta(\hat{s}+\hat{t}+\hat{u}) \,.
\end{aligned}
$$

- Hard factors H for the partonic subprocess $ab \to c$ for UU and UT.
- The transveristy PDF h_1^a and unpolarized PDF f.
- The OPEC FJFs $\mathcal{J}^c$ and $\mathcal{J}^c_{1,\perp}$.

Kinematics of OPEC Hadron in Jet

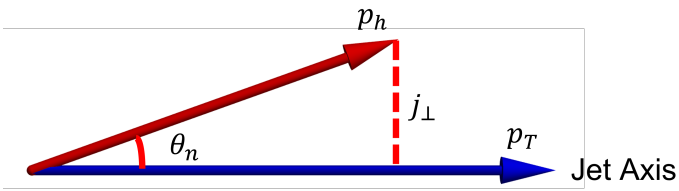

- The geometry yields

$$p_h^z = |\boldsymbol{p}_J| z_h = |\boldsymbol{p}_h| \cos\theta_n,$$

- In the collinear limit, we further see:

$$\theta_n \approx \sin\theta_n = \frac{j_\perp}{p_h^z} = \frac{j_\perp}{p_T z_h},$$

- Note in the centra rapidity, jet $|\boldsymbol{p}_J| = p_T$.

$j_\perp$ or θ_n?

- Compared with standard non-weighted TMD analysis, we have a different overall factor

$$z_h \, \mathrm{d}j_\perp^2 = p_T^2 \, z_h^3 \, \mathrm{d}\theta_n^2,$$

due to $j_\perp \simeq p_T z_h \theta_n$ in the collinear limit.

Why switch to θ_n?

- In one STAR configuration,
  - $\sqrt{s} = 510\,\mathrm{GeV}$, $p_T = 32.3\,\mathrm{GeV}$,
  - at lower cut $z = 0.1$,
  - $j_\perp$ can be measured in about (0.1, 1) GeV.
- $j_\perp$ only corresponds to θ_n about $(0.03, 0.3)$ rad.

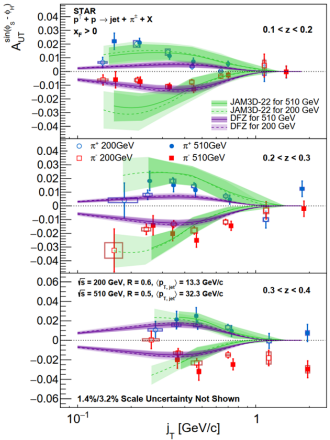

STAR collaboration arXiv.2507.16355

$j_\perp$ or θ_n?

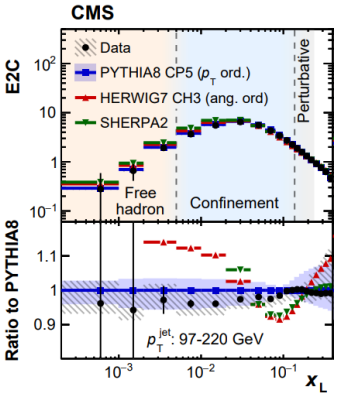

CMS (2024)

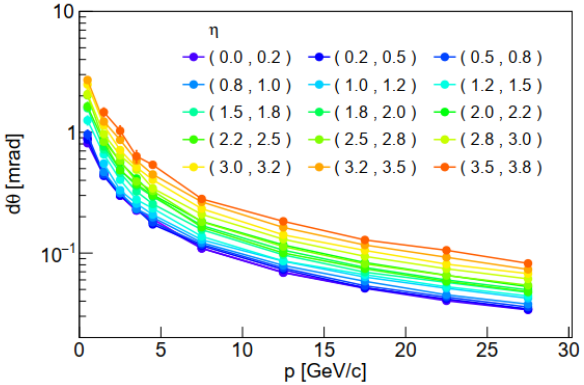

J. Arrington et al., EIC (2021)

- However, modern colliders could achieve angular resolution at 1 mrad!

TMD Evolution and Operator Product Expansion

- In the perturbative limit, the OPEC FJFs can be matched onto their collinear counterparts using the operator product expansion (OPE) and TMD evolution

$$\begin{aligned}\mathcal{J}^q(\theta_n, Q) =& \sum_h \int_0^1 \mathrm{d}z_h z_h \int_0^\infty \frac{\mathrm{d}b\, b}{2\pi} J_0\left(p_T \theta_n b\right) \\ & \times \hat{C}^D_{i\leftarrow q} \otimes D_{h/i}(z_h, \mu_b) e^{-\frac{1}{2} S_{\mathrm{pert}}(Q,b)}, \\ p_T \theta_n \mathcal{J}^q_{1,\perp}(\theta_n, Q) =& \sum_h \int_0^1 \mathrm{d}z_h z_h \int_0^\infty \frac{\mathrm{d}b\, b^2}{2\pi} J_1\left(p_T \theta_n b\right) \\ & \times \delta \hat{C}^{\mathrm{collins}}_{i\leftarrow q} \otimes \hat{H}^{T(1)}_{1\, h/i}(z_h, \mu_b) e^{-\frac{1}{2} S_{\mathrm{pert}}(Q,b)},\end{aligned}$$

- The usual convolution $\otimes$ is defined as

$$\hat{C}_{i\leftarrow q} \otimes F_{h/i} = \sum_i \int_{z_h}^1 \frac{\mathrm{d}z'_h}{z'_h} F_{h/i}(z'_h, \mu_b) \hat{C}_{i\leftarrow q}\left(\frac{z_h}{z'_h}, \mu_b, R\right).$$

Phenomenology Study on Energy-Weighted $\pi^{\pm}$ Production in Jet

- The OPEC Collins azimuthal asymmetry is defined as

$$A_{UT}^{\sin(\phi_s-\phi_n)} = \frac{Z_{UT}}{Z_{UU}}.$$

- We consider pion production in jets for two kinematic settings extensively studied by the STAR Collaboration:
  - (a) $\sqrt{s} = 510\,\text{GeV}$, $p_T = 32.3\,\text{GeV}$;
  - (b) $\sqrt{s} = 200\,\text{GeV}$, $p_T = 13.3\,\text{GeV}$.

Evaluation Frameworks

We present evaluation in two approaches:

- A full TMD evolution framework
  - Parametrization of the transversity PDF, Collins functions, and non-perturbative Sudakov factor from Kang, Prokudin, Sun, Yuan (2016) ,
  - The extraction is done for SIDIS and e^+e^- annhilation,
  - The application on $p^{\uparrow}p$ collision can be a complementary test of the TMD universality.
- The JAM3D-22 global QCD analysis: JAM (2022)
  - The TMD functions are modeled by Gaussian ansätze,
  - The corresponding collinear components evolve with only DGLAP.

p_T Distribution of the OPEC Collins Asymmetry

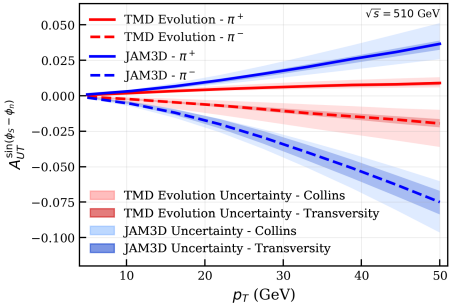

- JAM3D analysis gives overall larger Collins asymmetry than the TMD evolution framework.
- The error propagated from the parametrization of the Collins function is larger than from the transversity PDF.
- θ_n is integrated on (0, 0.1).

θ_n Distribution of the OPEC Collins Asymmetry

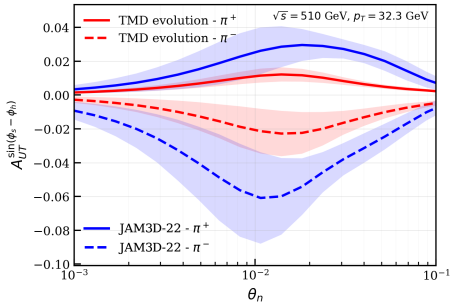

(a) $\sqrt{s} = 510$ GeV, $p_T = 32.3$ GeV

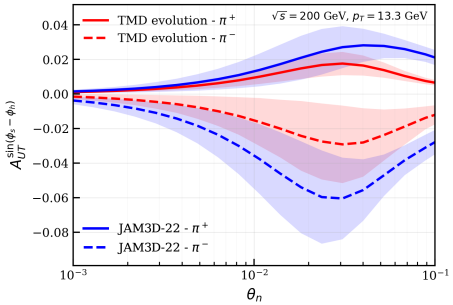

(b) $\sqrt{s} = 200$ GeV, $p_T = 13.3$ GeV

- Error is estimated from transversity PDF and Collins function combined.
- Two scenarios differ on the positions of their peak in θ_n.
- Current parametrizations do not yet allow us to resolve the effects of TMD evolution.

θ_n Distribution of the OPEC Collins Asymmetry for Different Weights

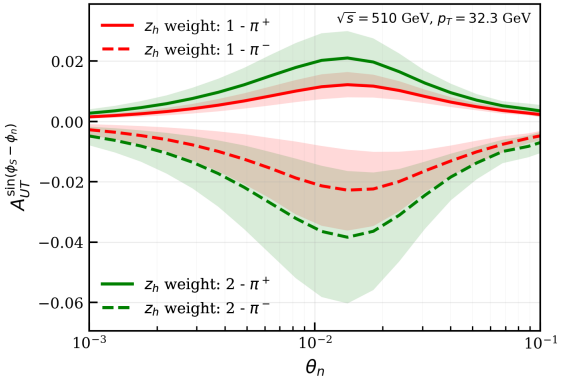

- Consistently enhancement of the Collins asymmetry for a higher power of the weight z_h (i.e. higher Mellin moment).

Conclusion

- We propose the one-point energy correlator (OPEC) for inclusive jet production in transversely polarized $p^{\uparrow}p$ collisions, sensitive to the transverse polarization effect through a $\sin(\phi_s - \phi_n)$ modulation.
- Compared with standard TMD studies, OPEC has two major benefits on determination of the transversity distribution:
  - The model dependency on final state fragmentation is reduced by taking the Mellin moment of the FJF.
  - OPEC estimates the Collins asymmetry by energy flow polar angle θ_n, accessing a much broader kinematic range of the jet substructure.
- We present a phenomenology study on $\pi^{\pm}$ production in jet.

Motivation for Hemisphere EEC

- Azimuthal asymmetry is not unique from polarization effects.
- **Soft recoil could also induce azimuthal asymmetry!**
  S. Catani, M. Grazzini, and A. Torre, 2014.
- Depending on kinematics, azimuthal asymmetry from soft recoil may even compete or even exceed those from polarization effects.
  Y. Hatta, B.W. Xiao, F. Yuan, and J. Zhou, 2021.

$$
\begin{aligned}
\mathcal{F}_{UU,T} &= \mathcal{P}[\tilde{f}_1^{(0)}\ \tilde{D}_1^{(0)}]\,, \\
\mathcal{F}_{UT,T}^{\sin(\phi_h-\phi_S)} &= -\mathcal{P}[\tilde{f}_{1T}^{\perp(1)}\ \tilde{D}_1^{(0)}]\,, \\
\mathcal{F}_{LL} &= \mathcal{P}[\tilde{g}_{1L}^{(0)}\ \tilde{D}_1^{(0)}]\,, \\
\mathcal{F}_{LT}^{\cos(\phi_h-\phi_s)} &= \mathcal{P}[\tilde{g}_{1T}^{(1)}\ \tilde{D}_1^{(0)}]\,, \\
\mathcal{F}_{UT}^{\sin(\phi_h+\phi_S)} &= \mathcal{P}[\tilde{h}_1^{(0)}\ \tilde{H}_1^{\perp(1)}]\,, \\
\mathcal{F}_{UU}^{\cos(2\phi_h)} &= \mathcal{P}[\tilde{h}_1^{\perp(1)}\ \tilde{H}_1^{\perp(1)}]\,, \\
\mathcal{F}_{UL}^{\sin(2\phi_h)} &= \mathcal{P}[\tilde{h}_{1L}^{\perp(1)}\ \tilde{H}_1^{\perp(1)}]\,, \\
\mathcal{F}_{UT}^{\sin(3\phi_h-\phi_S)} &= \frac{1}{4}\mathcal{P}[\tilde{h}_{1T}^{\perp(2)}\ \tilde{H}_1^{\perp(1)}].
\end{aligned}
$$

Azimuthal modulations at Leading twist in SIDIS,
D. Boer, L. Gamberg, B. Musch and A. Prokudin, 2011

Soft Recoil and Non-global logarithm (NGL)

- Non-global effects arise due to restricted phase space (e.g. jet, hemispheres) and consequently from the incomplete cancellation of the soft and collinear divergences.

  M. Dasgupta, G. P. Salam, 2001.

  R.B. Appleby and M.H. Seymour, 2002.

- In the large N_C limit, the LL NGLs evolution obeys the BMS equation.

  A. Banfi, G. Marchesini, and G. Smye, 2002.

- **NGLs contribute to typical observables on top of global logs**. For instance, in the dijet case, NGLs start appearing at $\mathcal{O}(\alpha_s^2)$ in the soft function.

  R. Kelley, M. D. Schwartz, R. M. Schabinger, and H. X. Zhu, 2011,
  A. Hornig, D. Kang, Y. Makris, and T. Mehen, 2017.

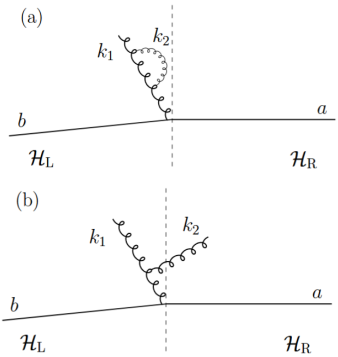

Figure from M. Dasgupta, G. P. Salam, 2001.

Hemisphere EEC

- We define the hemisphere EEC

$$\begin{aligned}&\mathrm{EEC}^{\mathrm{hemi}}(\theta_L,\,\theta_R,\,\phi)\\&=\int\frac{\mathrm{d}\phi_L\mathrm{d}\phi_R\,\mathrm{d}^2\boldsymbol{b}_L\mathrm{d}^2\boldsymbol{b}_R}{(2\pi)^4}\delta(\phi-\phi^q_{LR})H_{q\bar{q}}(Q)\\&\quad\times e^{\mathrm{i}\hat{\boldsymbol{q}}_L\cdot\boldsymbol{b}_L\theta_LQ/2}e^{\mathrm{i}\hat{\boldsymbol{q}}_R\cdot\boldsymbol{b}_R\theta_RQ/2}\,\mathcal{S}\,(\boldsymbol{b}_L,\boldsymbol{b}_R)J_q(b_L)\,J_{\bar{q}}(b_R)\end{aligned}$$

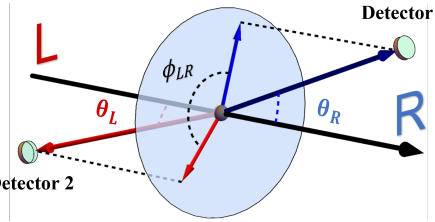

- with θ_L, θ_R the polar angle for the energy flows with respect to the thrust axis, ϕ^q_{LR} the azimuthal difference on the transverse plane.
- It is customary to take L the light side, and R the heavy side.
- The EEC jet function is

$$J_q(b,\mu)=\sum_h\int_0^1\mathrm{d}z\,z\,D_{h/q}(z,b,\mu).$$

TMD two-loop hemisphere soft function

- The soft function is

$$\tilde{S}\left(\boldsymbol{q}_L, \boldsymbol{q}_R\right) = \frac{1}{N_c} \sum_{X_s} \mathrm{Tr} \left\langle 0 \left| S_n^\dagger S_{\bar{n}} \right| X_s \right\rangle \langle X_s | S_{\bar{n}}^\dagger S_n | 0 \rangle \, \delta \left(\boldsymbol{q}_L - \sum_{i \in L} \boldsymbol{k}_i^T \right) \delta \left(\boldsymbol{q}_R - \sum_{j \in R} \boldsymbol{k}_j^T \right),$$

  where Wilson lines S_n, $S_{\bar{n}}$ are oriented along the two jet directions n and $\bar{n}$.

- Following the calculation strategy in G. Bell, R. Rahn, and J. Talbert, 2019, 2020, we compute the TMD two-loop hemisphere soft function

$$\mathcal{S}^{(2)}(b_L, b_R) = \mathcal{S}^{(2)}_{CF^2} + \mathcal{S}^{(2)}_{C_F C_A} + \mathcal{S}^{(2)}_{C_F n_f T_F},$$

  (with detailed results in the back-up slides).

ϕ^b_{LR} and $r = b_L/b_R$ Dependencies

- We find ϕ^b_{LR} and $r = b_L/b_R$ dependencies only in the non-singular terms.

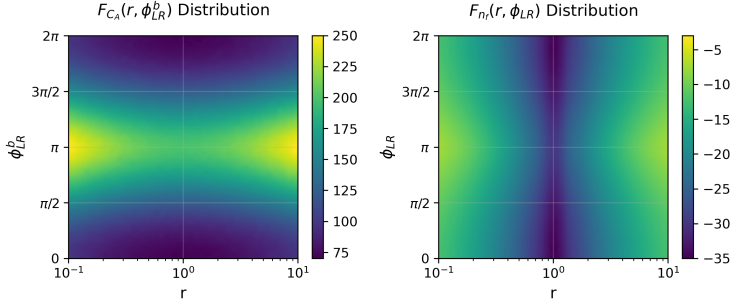

The $C_F C_A$ structure is much more dominant.

- The ϕ^b_{LR} dependency is a non-trivial structure from the non-global effects, as it persists in the non-global limit $r \to 0$ or $r \to \infty$.

Refactorization of the Non-global logarithm (NGL)

- The ϕ_{LR}^{b} dependency can be also predicted by the refactorization framework in the non-global limit.
  A. J. Larkoski, I. Moult, and D. Neill, 2015,
  T. Becher, M. Neubert, L. Rothen, and D. Y. Shao, 2015,
  S. Caron-Huot, 2015,
  T. Becher, B. D. Pecjak, and D. Y. Shao, 2016.
- The soft function is further factorized

$$\mathcal{S}\left(\boldsymbol{b}_L, \boldsymbol{b}_R\right) = \sum_{m=0}^{\infty} \left\langle \boldsymbol{\mathcal{H}}_m^S\left(\{\underline{n}\}, \boldsymbol{b}_R\right) \otimes \boldsymbol{\mathcal{S}}_{m+1}\left(\{\underline{n}\}, \boldsymbol{b}_L\right) \right\rangle,$$

The convolution $\otimes$ represents an angular integration over the directions of hard partons $\{\underline{n}\} = \{n_1, n_2, \ldots, n_m\}$. The refactorization separates a "harder" soft function $\boldsymbol{\mathcal{H}}_m^S$ from a "softer" function $\boldsymbol{\mathcal{S}}_{m+1}$, corresponding to configurations with m hard partons.

Refactorization of the Non-global logarithm (NGL)

- The "harder" function is defined as

$$\boldsymbol{\mathcal{H}}_m^S\left(\{\underline{\mathrm{n}}\},\boldsymbol{b}_R\right)=\int d^{d-2}\boldsymbol{q}_R\prod_{i=1}^m\int\frac{dE_iE_i^{d-3}}{(2\pi)^{d-2}}\theta_R\left(\{\underline{\mathrm{p}}\}\right)\left|\mathcal{M}_m^S\left\{\underline{\mathrm{p}}\right\}\right\rangle\left\langle\mathcal{M}_m^S\left\{\underline{\mathrm{p}}\right\}\right|\delta\left(\boldsymbol{q}_R-\boldsymbol{P}_{sT}^R\right)e^{i\boldsymbol{q}_R\cdot\boldsymbol{b}_R}$$

where $\{\underline{n}\}$ and $\{\underline{p}\}$ denote the directions and momenta of the Wilson lines. The constraint $\theta_R(\{\underline{p}\})=\theta_R(p_1)\theta_R(p_2)\cdots\theta_R(p_m)$ restricts the hard emissions to hemisphere R, and $\boldsymbol{P}_{sT}^R$ is the sum of transverse momenta of real-emission partons in R. The color-space amplitude is

$$\left|\mathcal{M}_m^S\left\{\underline{\mathrm{p}}\right\}\right\rangle=\left\langle\left\{\underline{\mathrm{p}}\right\}\left|S_nS_{\bar{n}}^\dagger\right|0\right\rangle$$

with Wilson line S_{n_i} along the corresponding direction n_i.

- The "softer" function is defined

$$\boldsymbol{\mathcal{S}}_{m+1}\left(\{\underline{\mathrm{n}}\},\boldsymbol{b}_L\right)=\int d^{d-2}\boldsymbol{q}_L\delta\left(\boldsymbol{q}_L-\boldsymbol{P}_{sT}^L\right)e^{i\boldsymbol{q}_L\cdot\boldsymbol{b}_L}\sum_X\left|\left\langle0\left|S_{a,\bar{n}}^\dagger S_{b,n}^\dagger S_{1,n_1}^\dagger\cdots S_{m,n_m}^\dagger\right|X\right\rangle\right|^2$$

Azimuthal Asymmetries from soft function

- The non-singular term given by the refactorized calculation of the $C_F C_A$ color structure.
- Unlike spin-induced asymmetries, it does not have a fixed angular modulation. The asymmetry from recoil apply to $\cos(n\phi^b_{LR})$ for $n = 1, 2, \ldots, \infty$.

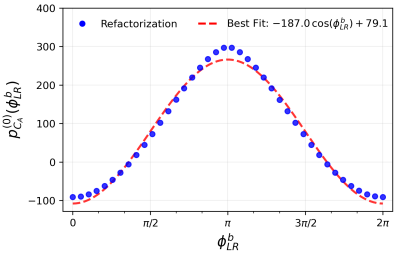

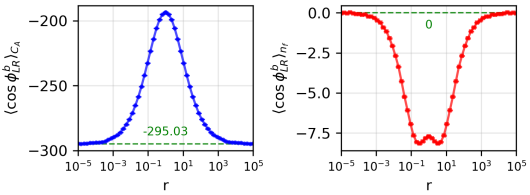

- We define the hemisphere azimuthal projection

$$\langle \cos n\phi^b_{LR} \rangle = \int_0^{2\pi} \mathrm{d}\phi^b_{LR}\, \cos(n\phi^b_{LR})\, f(\phi^b_{LR})\,,$$

The full TMD asymmetries (blue, red) agree with the refactorized calculation (green dashed line).

Azimuthal Asymmetries from soft function

- We consider hemisphere EEC azimuthal projection in the momentum space

$$\langle \cos(n\phi) \rangle_{\theta_L \theta_R} \equiv \frac{1}{\sigma_0} \int_0^{2\pi} \mathrm{d}\phi_L^q \mathrm{d}\phi_R^q \cos\left(n\phi_{LR}^q\right) \times \mathrm{EEC}^{\mathrm{hemi}}(\theta_L, \theta_R, \phi_{LR}^q)$$

- For phenomenological applications, we define the cumulative azimuthal projection integrated over θ_R:

$$\langle \cos(n\phi) \rangle_{\theta_L} = \int_{\theta_{\min}}^{\theta_{\max}} \mathrm{d}\theta_R \langle \cos(n\phi) \rangle_{\theta_L \theta_R},$$

and compare the differential distribution on the $\log_{10}\theta_L$ with EVENT2 simulations, using 3×10^{10} events and a cutoff of 10^{-24}.

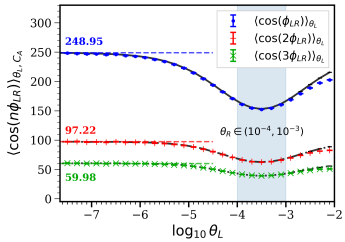

Azimuthal Asymmetries with TMD Resummation

- We define the hemisphere EEC azimuthal asymmetry as

$$A_{n,\theta_L}^{\text{Hemi}} = \frac{\langle \cos(n\phi) \rangle_{\theta_L}}{\langle \Sigma \rangle_{\theta_L}}$$

with the denominator without azimuthal modulation

$$\begin{aligned}
\langle \Sigma \rangle_{\theta_L} &= \int_{\theta_{\min}}^{\theta_{\max}} \mathrm{d}\theta_R \frac{1}{\sigma_0} \frac{\mathrm{d}\Sigma}{\mathrm{d}\log\theta_L} \\
&= \int_{\theta_{\min}}^{\theta_{\max}} \mathrm{d}\theta_R \int \mathrm{d}b_L \mathrm{d}b_R \, b_L b_R \, H_{q\bar{q}} J_q(b_L) J_{\bar{q}}(b_R) \mathcal{S}(b_L, b_R) \\
&\quad \times J_0\left(b_L \theta_L \frac{Q}{2}\right) e^{-S_{\text{pert}}(b_L,Q) - S_{\text{NP}}(b_L,Q)} \, J_0\left(b_R \theta_R \frac{Q}{2}\right) e^{-S_{\text{pert}}(b_R,Q) - S_{\text{NP}}(b_R,Q)}
\end{aligned}$$

- We take the EEC jet function at LO $J_q = J_{\bar{q}} = 1$, and the hard function $H_{q\bar{q}} = 1$.
- We use the non-perturbative Sudakov factor fitted using EEC input.

Z.B. Kang, J. Penttala, and C. Zhang, 2024.

Azimuthal Asymmetry with TMD Resummation

- We get the azimuthal asymmetry with TMD resummation
- The asymmetries increase with both larger θ_L and higher Q, reflecting enhanced recoil from soft gluon emissions carrying larger transverse momenta at wider angles and higher center-of-mass energy.

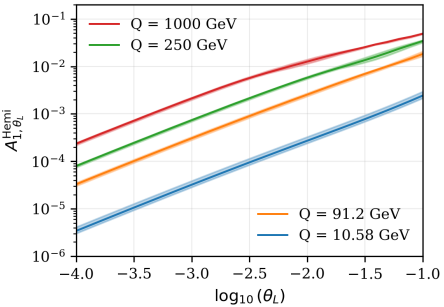

- Notably, the asymmetry $A^{\mathrm{Hemi}}_{n,\theta_L}$ probes TMD in b space dominated by the J_1 Bessel mode, which in conventional TMD observables appears only in polarized channels. It also provides a new, distinct channel to examine the TMD universality.
- Higher harmonics associated with $J_{n\geq 2}$ also emerge naturally within this construction.

Conclusion

- We proposed the hemisphere EEC in e^+e^- annihilation as a new observable that directly exposes the non-global structure of QCD radiation.
- We compute the 2-loop hemisphere functions both in full TMD theory and refactorized calculation.
- By correlating energy flow between opposite hemispheres, it isolates azimuthal patterns generated purely by soft-gluon recoil, providing a clean handle on non-global dynamics that have so far been accessible only indirectly.

Backup: OPEC FJF Factorization

- Analogously to the TMD FJFs (Z.B. Kang, X. Liu, F. Ringer, and H. Xing, 2017; Z.B. Kang, K. Lee, and F. Zhao, 2020), the OPEC FJFs admit the factorized representations in the limit $R \gg \theta_n$,

$$\begin{aligned}\mathcal{J}^c(z,\hat{\boldsymbol{n}},\omega_J R,\mu) =& \mathcal{H}_{c\to i}(z,\omega_J R,\mu)\int \mathrm{d}^2\boldsymbol{l}_\perp \mathrm{d}^2\boldsymbol{\lambda}_\perp \delta^2\left(\boldsymbol{l}_\perp + p_T\theta_n\hat{\boldsymbol{n}}_T - \boldsymbol{\lambda}_\perp\right)\\ &\times J_i^U(\boldsymbol{l}_\perp,\mu,\nu) S_i(\boldsymbol{\lambda}_\perp,\mu,\nu R)\ ,\\ p_T\theta_n\mathcal{J}^q_{1,\perp}(z,\hat{\boldsymbol{n}},\omega_J R,\mu) =& \mathcal{H}^T_{c\to i}(z,\omega_J R,\mu)\int \mathrm{d}^2\boldsymbol{l}_\perp \mathrm{d}^2\boldsymbol{\lambda}_\perp \delta^2\left(\boldsymbol{l}_\perp + p_T\theta_n\hat{\boldsymbol{n}}_T - \boldsymbol{\lambda}_\perp\right)\\ &\times p_T\theta_n J_i^T(\boldsymbol{l}_\perp,\mu,\nu) S_i(\boldsymbol{\lambda}_\perp,\mu,\nu R)\ .\end{aligned}$$

- $\mathcal{H}$ is a hard matching coefficient, encodes the contributions from radiations at the jet scale $\omega_J R$. J is the OPEC jet function.

Backup: OPEC jet function OPE

The z^{N-1} OPEC jet function can be matched on to the collinear counterparts

$$\tilde{J}_q^U(\boldsymbol{b},\mu,\nu) = C_{qq}(\boldsymbol{b},\mu,\nu)\,\tilde{D}^N_{q/q}(\mu) + C_{gq}(\boldsymbol{b},\mu,\nu)\,\tilde{D}^N_{g/q}(\mu),$$
$$\tilde{J}_g^U(\boldsymbol{b},\mu,\nu) = C_{gg}(\boldsymbol{b},\mu,\nu)\,\tilde{D}^N_{g/g}(\mu) + C_{qg}(\boldsymbol{b},\mu,\nu)\,\tilde{D}^N_{q/g}(\mu),$$
$$\tilde{J}_q^T(\boldsymbol{b},\mu,\nu) = \delta C_{qq}(\boldsymbol{b},\mu,\nu)\,\tilde{H}^{(3)N}_{q/q}(\mu),$$

with the NLO renormalized matching coefficients

$$C_{qq}(\boldsymbol{b},\mu,\nu) = 1 + \frac{\alpha_s}{2\pi}\left[C_F\left(\ln\frac{\mu^2}{\mu_b^2}\left(\frac{3}{2}+2\ln\frac{\nu}{\omega_J}\right)+\frac{1}{N(N+1)}\right) - \gamma_{qq}(N)\ln\frac{\mu^2}{\mu_b^2} - 2\gamma^{(1)}_{qq}(N)\right],$$
$$C_{gq}(\boldsymbol{b},\mu,\nu) = \frac{\alpha_s}{2\pi}\left[-\gamma_{gq}(N)\ln\frac{\mu^2}{\mu_b^2} - 2\gamma^{(1)}_{gq}(N) + C_F\frac{1}{N+1}\right],$$
$$C_{gg}(\boldsymbol{b},\mu,\nu) = 1 + \frac{\alpha_s}{2\pi}\left[C_A\ln\frac{\mu^2}{\mu_b^2}\left(\frac{\beta_0}{2C_A}+2\ln\frac{\nu}{\omega_J}\right) - \gamma_{gg}(N)\ln\frac{\mu^2}{\mu_b^2} - 2\gamma^{(1)}_{gg}(N)\right],$$
$$C_{qg}(\boldsymbol{b},\mu,\nu) = \frac{\alpha_s}{2\pi}\left[-\gamma_{qg}(N)\ln\frac{\mu^2}{\mu_b^2} - 2\gamma^{(1)}_{qg}(N) + T_F\frac{2}{(N+1)(N+2)}\right],$$
$$\delta C_{qq}(\boldsymbol{b},\mu,\nu) = 1 + \frac{\alpha_s}{2\pi}\left[C_F\ln\frac{\mu^2}{\mu_b^2}\left(\frac{3}{2}+2\ln\frac{\nu}{\omega_J}\right) - \Delta_T\gamma_{qq}(N)\ln\frac{\mu^2}{\mu_b^2} - 2\Delta_T\gamma^{(1)}_{qq}(N)\right].$$

Backup: Scale uncertainties

- For the TMD evolution framework, we vary both the OPE scale μ_i and the hard scale $\mu = Q$ independently by a factor of two around their canonical values ($\mu_i = \mu_{b^*}$ and $\mu = Q = p_T$) to estimate the perturbative uncertainty.
- For the JAM3D-based approach, where only collinear DGLAP evolution is included, we vary the hard scale $\mu = Q = p_T$ in the same manner.

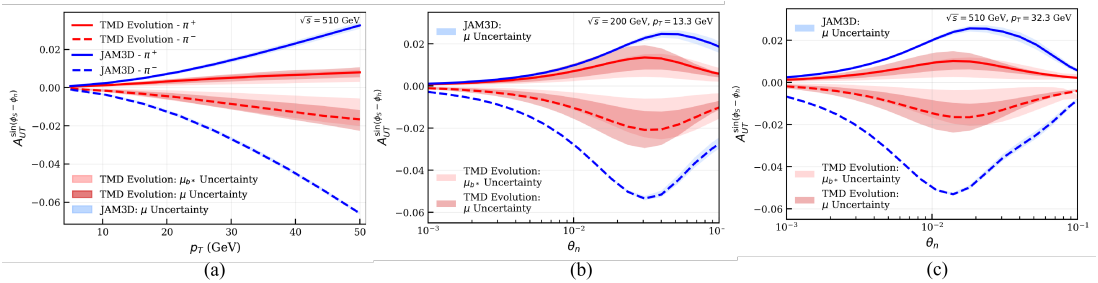

Backup: 2-loop TMD soft function

- The bare 2-loop TMD soft function is

$$\begin{aligned}\mathcal{S}^{(2)}\left(\boldsymbol{b}_L,\boldsymbol{b}_R\right)=&\left(\frac{\alpha_s}{4\pi}\right)^2\left[\left(\mu b_L\right)^{4\epsilon}\left(\nu b_L\right)^{\alpha}+\left(\mu b_R\right)^{4\epsilon}\left(\nu b_R\right)^{\alpha}\right]\left[\left(\nu b_{L,R}\right)^{\alpha}\frac{C_F^2h_F^2}{2}+C_FC_A\left(h_A+v_A\right)+C_FT_Fn_fh_f\right]\\&+\left(\frac{\alpha_s}{4\pi}\right)^2\left[\left(\mu b_L\right)^{4\epsilon}\left(\nu b_L\right)^{\alpha}+\left(\mu b_R\right)^{4\epsilon}\left(\nu b_R\right)^{\alpha}\right]\frac{\beta_0}{\epsilon}h_F\\&+\left(\frac{\alpha_s}{4\pi}\right)^2\left(\mu b_L\right)^{2\epsilon}\left(\mu b_R\right)^{2\epsilon}\left[C_FC_Ag_A\left(r,\theta_{LR}\right)+\left(\nu b_L\right)^{\alpha}\left(\nu b_R\right)^{\alpha}C_F^2p_F+C_Fn_fT_Fg_f\left(r\right)\right]\end{aligned}$$

- First line: two real emissions in the same hemisphere (with virtual correction v_A).
- Second line: running coupling.
- Third line: two real emissions in opposite hemispheres.

Backup: 2-loop TMD soft function

- The detailed expressions of the configuration two real emissions in the same hemisphere and the virtual virtual correction to single-gluon emission,

$$
\begin{aligned}
h_F =& -\frac{2}{\epsilon^2}+\frac{4}{\alpha\epsilon}+\frac{\alpha}{\epsilon^3}+\frac{\pi^2}{6}-\frac{\pi^2}{4}\frac{\alpha}{\epsilon}+\frac{\pi^2}{3}\frac{\epsilon}{\alpha}+\frac{\zeta_3}{3}\alpha+\frac{4\zeta_3}{3}\left(\epsilon+\frac{\epsilon^2}{\alpha}\right)+\frac{3\pi^4}{80}\epsilon^2+\frac{9\zeta_4}{4}\frac{\epsilon^3}{\alpha}-\frac{\pi^4}{480}\alpha\epsilon,\\
h_A =& \frac{1}{\epsilon^4}+\frac{11}{6\epsilon^3}-\frac{4}{\alpha\epsilon^3}-\frac{22}{3\alpha\epsilon^2}+\left(\frac{67}{18}-\pi^2\right)\frac{1}{\epsilon^2}-\frac{2}{9}\left(67-6\pi^2\right)\frac{1}{\alpha\epsilon}+\left(\frac{211}{27}-\frac{77}{36}\pi^2-\frac{61}{3}\zeta_3\right)\frac{1}{\epsilon}\\
&-\frac{1}{27}\left(808+33\pi^2-684\zeta_3\right)\frac{1}{\alpha}-66.45(57),\\
h_f =& -\frac{2}{3\epsilon^3}+\frac{8}{3\alpha\epsilon^2}-\frac{10}{9\epsilon^2}+\frac{40}{9\alpha\epsilon}+\frac{4}{27}\left(56+3\pi^2\right)\frac{1}{\alpha}-\left(\frac{74}{27}-\frac{7}{9}\pi^2\right)\frac{1}{\epsilon}+24.7282(19),\\
v_A =& -\frac{1}{\epsilon^4}+\frac{4}{\alpha\epsilon^3}+\frac{\pi^2}{2\epsilon^2}-\frac{2\pi^2}{3\alpha\epsilon}+\frac{28\zeta_3}{3\epsilon}+\frac{8\zeta_3}{3\alpha}+\frac{57}{4}\zeta_4.
\end{aligned}
$$

Backup: 2-loop TMD soft function

- The contribution in which the two emissions populate opposite hemispheres. This is the origin of non-global dynamics and induces dependence on the ratio $r = b_L/b_R$ and on the relative azimuthal angle ϕ^b_{LR} between $\boldsymbol{b}_L$ and $\boldsymbol{b}_R$.

$$
\begin{aligned}
p_F &= \frac{12}{\epsilon^4} - \frac{16}{\alpha\epsilon^3} + \frac{16}{\alpha^2\epsilon^2} + \frac{8\pi^2}{3\alpha^2} - \frac{2\pi^2}{\epsilon^2} + \frac{16\zeta_3}{3\alpha} - \frac{43\pi^4}{180}, \\
g_A &= \frac{2\pi^2}{3\epsilon^2} + \frac{1}{\epsilon}\left(-\frac{2}{3} + \frac{22\pi^2}{9} + 8\zeta_3\right) + \frac{4}{9}\left(3 - 11\pi^2 + 18\zeta_3\right)\log(r) \\
&\quad + \frac{16}{9} - \frac{134\pi^2}{27} + \frac{2\pi^4}{45} + \frac{176\zeta_3}{3} + F_{C_A}(r, \theta_{LR}), \\
g_f &= \frac{1}{\epsilon}\left(\frac{4}{3} - \frac{8\pi^2}{9}\right) + \frac{8}{9}\left(-3 + 2\pi^2\right)\log(r) - \frac{20}{9} + \frac{64\pi^2}{27} - \frac{64}{3}\zeta_3 + F_{n_f}(r, \theta_{LR}),
\end{aligned}
$$

Backup: 2-loop TMD soft function

- we obtain the renormalized two-loop TMD hemisphere soft function

$$\mathcal{S}^{(2)}(b_L, b_R) = \mathcal{S}^{(2)}_{C_F^2} + \mathcal{S}^{(2)}_{C_F C_A} + \mathcal{S}^{(2)}_{C_F n_f T_F} ,$$

with each color structure

$$\begin{aligned}
S^{(2)}_{C_F^2} &= \frac{1}{2}\left[L_L^2 + L_R^2 + \frac{\pi^2}{3} + 4\,(L_L + L_R)\log\left(\frac{\nu}{\mu}\right)\right]^2 , \\
S^{(2)}_{C_F C_A} &= -\frac{22}{9}\left(L_L^3 + L_R^3\right) - \frac{67}{9}\left(L_L^2 + L_R^2\right) - \frac{11\pi^2}{9}\left(L_L + L_R\right) + \frac{2\pi^2}{3} L_L L_R + \left(\frac{4}{3} - \frac{44}{9}\pi^2 + 8\zeta_3\right)\log r \\
&\quad + \left[-\frac{22}{3}\left(L_L^2 + L_R^2\right) - \left(\frac{268}{9} - \frac{4}{3}\pi^2\right)\left(L_L + L_R\right) - \frac{8}{27}\left(202 - 189\zeta_3\right)\right]\log\left(\frac{\nu}{\mu}\right) \\
&\quad - 62.7(11) + F_{CA}\left(r, \theta_{LR}\right) , \\
S^{(2)}_{C_F n_f T_F} &= \frac{8}{9}\left(L_L^3 + L_R^3\right) + \frac{20}{9}\left(L_L^2 + L_R^2\right) + \frac{4\pi^2}{9}\left(L_L + L_R\right) + \left(\frac{16}{9}\pi^2 - \frac{8}{3}\right)\log r + 40.75(8) \\
&\quad + \left[\frac{8}{3}\left(L_L^2 + L_R^2\right) + \frac{80}{9}\left(L_L + L_R\right) + \frac{8}{27}\left(56 + 3\pi^2\right)\right]\log\left(\frac{\nu}{\mu}\right) + F_{nf}\left(r, \theta_{LR}\right) ,
\end{aligned}$$

with $L_L = \log(b_L \mu / 2e^{\gamma_E})$ and $L_R = \log(b_R \mu / 2e^{\gamma_E})$.

Backup: 2-loop TMD soft function from refactorization

- We compute the two-loop hemisphere soft function in the strongly asymmetric limit $b_R \gg b_L$ (i.e. $r = b_L/b_R \to 0$). In this limit the soft radiation at the hard scale $1/b_R$ can be separated from the softer mode at the scale $1/b_L$, and the result takes the form

$$\begin{aligned}\tilde{s}^{(2)}\left(\boldsymbol{b}_L, \boldsymbol{b}_R, \epsilon\right) = & \left[\left(\mu b_L\right)^{4\epsilon}\left(\nu b_L\right)^{\alpha} + \left(\mu b_R\right)^{4\epsilon}\left(\nu b_R\right)^{\alpha}\right]\left[\left(\nu b_{L,R}\right)^{\alpha} C_F^2 h_F^2/2 + C_F C_A\left(h_A + v_A\right) + C_F T_F n_f h_f\right] \\ & + \left[\left(\mu b_L\right)^{2\epsilon}\left(\nu b_L\right)^{\alpha} + \left(\mu b_R\right)^{2\epsilon}\left(\nu b_R\right)^{\alpha}\right]\frac{\beta_0}{\epsilon} h_F \\ & + \left(\mu b_L\right)^{4\epsilon}\left[C_F C_A\left(s_A - h_A - v_A\right) + C_F T_F n_f\left(s_f - h_f\right)\right] \\ & + \left(\mu b_L\right)^{2\epsilon}\left(\mu b_R\right)^{2\epsilon}\left[C_F C_A p_A + \left(\nu b_L\right)^{\alpha}\left(\nu b_R\right)^{\alpha} C_F^2 p_F\right]\end{aligned}$$

where the first two lines are computed exactly the same as in the standard TMD case.

Backup: 2-loop TMD soft function from refactorization

- The third line corresponds to the opposite-hemisphere contribution to the NNLO correction of the refactorized soft sector with an inclusive hard hemisphere. It can be obtained by taking the $b_R \to \infty$ limit in the standard TMD computation. We find

$$s_A - h_A - v_A = \frac{1}{\epsilon}\left(-\frac{2}{3} + \frac{22\pi^2}{9} - 4\zeta_3\right) + \frac{16}{9} - \frac{134\pi^2}{27} + \frac{176\zeta_3}{3} + \frac{2\pi^4}{45},$$
$$s_f - h_f = \frac{1}{\epsilon}\left(\frac{4}{3} - \frac{8\pi^2}{9}\right) - \frac{20}{9} + \frac{64\pi^2}{27} - \frac{64\zeta_3}{3}.$$

- The fourth line arises from configurations in which both the refactorized hard function and the soft function receive NLO corrections, schematically

$$\left\langle \tilde{\boldsymbol{\mathcal{H}}}_1^{S(1)} \otimes \tilde{\boldsymbol{\mathcal{S}}}_2^{(1)} \right\rangle = \int \frac{\mathrm{d}\Omega\left(n_1\right)}{4\pi}\, \boldsymbol{\mathcal{H}}_1^{S(1)}\left(\{n_1\}, \boldsymbol{b}_R\right) \boldsymbol{\mathcal{S}}_2^{(1)}\left(\{n_1\}, \boldsymbol{b}_L\right),$$

where $\mathrm{d}\Omega(n_1)$ denotes the solid-angle integration over the direction n_1 of the hard parton. Therefore, we obtain

$$p_F = \frac{12}{\epsilon^4} - \frac{16}{\alpha\epsilon^3} + \frac{16}{\alpha^2\epsilon^2} + \frac{8\pi^2}{3\alpha^2} - \frac{2\pi^2}{\epsilon^2} + \frac{16\zeta_3}{3\alpha} - \frac{43\pi^4}{180},$$
$$p_A = \frac{2\pi^2}{3\epsilon^2} + \frac{12\zeta_3}{\epsilon} + p_{C_A}^{(0)}\left(\phi_{LR}^b\right).$$

Backup: Fourier transform in the Asymmetry Evaluation

Using $\boldsymbol{q}_i \cdot \boldsymbol{b}_i = Q b_i \theta_i \cos(\phi_i^q - \phi_i^b)/2$ for $i = L, R$ and applying the Jacobi–Anger expansion, we obtain

$$\begin{aligned}\langle \cos(n\phi) \rangle_{\theta_L \theta_R} =& (-1)^n \left(\frac{\alpha_s}{4\pi}\right)^2 \frac{Q^4}{16} \int \mathrm{d}b_L^2 \mathrm{d}b_R^2 \; J_n\left(b_L \theta_L \frac{Q}{2}\right) \\ & \cdot J_n\left(b_R \theta_R \frac{Q}{2}\right) \int \frac{\mathrm{d}\phi_{LR}^b}{2\pi} \mathcal{S}^{(2)}\left(\frac{b_L}{b_R}, \phi_{LR}^b\right) \cos(n\phi_{LR}^b)\end{aligned}$$

where J_n is the Bessel function. We introduce the azimuthally projected b-space function

$$A_n^b(r) = \int_0^{2\pi} \mathrm{d}\phi_{LR}^b \cos(n\phi_{LR}^b) \mathcal{S}^{(2)}\left(r, \phi_{LR}^b\right),$$

which allows us to rewrite the asymmetry in closed analytical form in A_n^b as

$$\begin{aligned}\langle \cos(n\phi) \rangle_{\theta_L \theta_R} = \frac{(-1)^n}{2\pi} \left(\frac{\alpha_s}{4\pi}\right)^2 \Bigg[& \frac{n^2 A_n^b(\theta_L/\theta_R)}{\theta_L \theta_R} \\ & - \frac{{A_n^b}'(\theta_L/\theta_R)}{\theta_R^2} - \frac{\theta_L {A_n^b}''(\theta_L/\theta_R)}{\theta_R^3} \Bigg]\end{aligned}$$

where we used the symmetry $A_n^b(r) = A_n^b(1/r)$. One may verify that an inverse Hankel transform indeed reproduces the b-space kernel.